Zeeman response of d-wave superconductors: Born approximation for impurity and spin-orbit scattering potentials

2000 J. Phys.: Condens. Matter 12 1329

(http://iopscience.iop.org/0953-8984/12/7/316)

J. Phys.: Condens. Matter **12** (2000) 1329–1338. Printed in the UK PII: S0953-8984(00)07490-7

Zeeman response of d-wave superconductors: Born approximation for impurity and spin–orbit scattering potentials

Claudio Grimaldi

École Polytechnique Fédérale de Lausanne, Département de Microtechnique IPM, CH-1015 Lausanne, Switzerland

Received 3 September 1999

Abstract. The effects of impurity and spin–orbit scattering potentials can strongly affect the Zeeman response of a d-wave superconductor. Here, both the phase diagram and the quasiparticle density of states are calculated within the Born approximation and it is found that the spin–orbit interaction influences in qualitatively different ways the Zeeman responses of d-wave and s-wave superconductors.

1. Introduction

The layered structure of cuprates makes these materials good candidates for observing Zeeman response to a magnetic field $\boldsymbol{H}$ directed parallel to the Cu–O planes [1–3]. Moreover, the $\mathrm{d}_{x^2-y^2}$ symmetry of the order parameter (hereafter d wave) leads in principle to substantial differences with respect to the Zeeman response of isotropic s-wave superconductors. For example, at zero temperature, the tunnelling conductance $\sigma_s(0)$ of a d-wave superconductor–insulator–metal junction is non-zero for finite voltages V provided $\boldsymbol{H} \neq 0$ [1, 2], in sharp contrast to the case for ordinary isotropic s-wave junctions, for which $\sigma_s(0)$ is zero for $V < \Delta/e$, where Δ is the energy gap and e is the electron charge [4]. On the other hand, the phase diagrams of pure s-wave and d-wave superconductors in the presence of a Zeeman magnetic field have similar qualitative behaviours. For example, for both symmetries of the order parameter, a first-order phase transition to the normal state is found at low temperatures and for sufficiently strong magnetic fields [1, 5]. However, there are quantitative differences. For example, at $T = 0$, the critical field is $\mu_{\mathrm{B}} H_{\mathrm{c}}/\Delta_0 = 1/\sqrt{2}$ for s waves [5, 6] and $\mu_{\mathrm{B}} H_{\mathrm{c}}/\Delta_0 \simeq 0.56$ for d waves [1, 2], where Δ_0 is the zero-temperature order parameter without magnetic field and μ_{B} is the Bohr magneton.

So far, systematic theoretical studies of the Zeeman response of anisotropic superconductors have been focused on the clean limit of the d-wave BCS formulation [1–3]. A more realistic situation would require the inclusion of impurity effects, since these are known to have important effects on both thermodynamic and spectral quantities [7]. Moreover, in addition to the disorder potential, the quasiparticles are also spin–orbit coupled to the impurities, so the Zeeman response is affected by spin-mixing processes. An additional source for spin–orbit effects could be provided by the electric fields in the vicinity of the conducting Cu–O layers and the charge reservoir interfaces.

0953-8984/00/071329+10$30.00

Although, in the past few years, the effect of spin–orbit coupling has been intensively studied for isotropic s-wave superconductors [4, 8], the corresponding situation for d-wave superconductors (or other anisotropic symmetries) is still unknown. However, it is expected that the spin–orbit effects on the Zeeman response of d-wave superconductors differ from those for s-wave superconductors in a qualitative way. In fact, even at zero magnetic field, the spin–orbit scattering is pair breaking and reduces both the critical temperature T_c and the order parameter [9]. As a consequence, for $H \neq 0$, the pair-breaking effects of the external magnetic field and the spin–orbit coupling add together. This situation must be contrasted with the s-wave case, where the spin–orbit potential is not pair breaking and competes with the Zeeman response, reducing the pair-breaking effect of the magnetic field [4].

In this paper, the effects of both impurity and spin–orbit scattering potentials are studied within a self-consistent Born approximation for d-wave superconductors. Both thermodynamic and spectral properties are investigated and compared with those of s-wave superconductors.

2. Born approximation

Let us consider a two-dimensional system with electrons (holes) moving in the x–y plane under the influence of an external magnetic field $\boldsymbol{H}$ directed along the plane. In this situation, the coupling of the orbital motion of the charge carriers to the magnetic field is vanishingly small. In the following, no particular pairing mechanism is assumed and the condensate will be described within the BCS formalism. In this framework, the Hamiltonian is

$$H_0 = \sum_{\boldsymbol{k},\alpha} \epsilon(\boldsymbol{k}) c^\dagger_{\boldsymbol{k}\alpha} c_{\boldsymbol{k}\alpha} - I \sum_{\boldsymbol{k}\alpha} \alpha c^\dagger_{\boldsymbol{k}\alpha} c_{\boldsymbol{k}\alpha} - \sum_{\boldsymbol{k}} \Delta(\boldsymbol{k})(c^\dagger_{\boldsymbol{k}\uparrow} c^\dagger_{-\boldsymbol{k}\downarrow} + c_{-\boldsymbol{k}\downarrow} c_{\boldsymbol{k}\uparrow}) \tag{1}$$

where $I = \mu_B H$ and μ_B is the Bohr magneton. For a $d_{x^2-y^2}$ symmetry of the gap, $\Delta(\boldsymbol{k})$ is parametrized as follows:

$$\Delta(\boldsymbol{k}) = \Delta \cos(2\phi) \tag{2}$$

where ϕ is the polar angle in the k_x–k_y plane. In equation (1), $\uparrow$ and $\downarrow$ refer to the spin directions along and opposite to the direction of $\boldsymbol{H}$, and it is assumed that $\boldsymbol{H}$ is directed along the x-direction, so that $\boldsymbol{H} = H\hat{\boldsymbol{x}}$.

The interaction Hamiltonian describing the coupling to the impurities located randomly at $\boldsymbol{R}_i$ is given below:

$$H' = v_{\rm imp} \sum_{\boldsymbol{k}\boldsymbol{k}'i} \sum_{\alpha} \mathrm{e}^{-\mathrm{i}(\boldsymbol{k}-\boldsymbol{k}')\cdot\boldsymbol{R}_i} c^\dagger_{\boldsymbol{k}\alpha} c_{\boldsymbol{k}'\alpha} + \mathrm{i}\frac{v_{\rm so}}{k_F^2} \sum_{\boldsymbol{k}\boldsymbol{k},i} \sum_{\alpha,\beta} \mathrm{e}^{-\mathrm{i}(\boldsymbol{k}-\boldsymbol{k}')\cdot\boldsymbol{R}_i} ([\boldsymbol{k}\times\boldsymbol{k}']\cdot\boldsymbol{\sigma}_{\alpha\beta}) c^\dagger_{\boldsymbol{k}\alpha} c_{\boldsymbol{k}'\beta} \tag{3}$$

where $v_{\rm imp}$ and $v_{\rm so}$ refer to the non-magnetic and spin–orbit coupling to the impurities, respectively (k_F is the Fermi momentum). From the Elliott relation [10], the impurity and spin–orbit potentials are roughly given by $v_{\rm so} \sim \Delta g\, v_{\rm imp}$, where Δg is the shift of the g-factor which, for cuprates, is of order 0.1. Here, however, $v_{\rm imp}$ and $v_{\rm so}$ will be treated as independent variables. Note that, since the momenta $\boldsymbol{k}$ and $\boldsymbol{k}'$ are defined in the x–y plane, the spin-momentum dependence of the spin–orbit interaction simplifies to

$$[\boldsymbol{k}\times\boldsymbol{k}']\cdot\boldsymbol{\sigma}_{\alpha\beta} = [\boldsymbol{k}\times\boldsymbol{k}']\cdot\hat{\boldsymbol{z}}\,\sigma^z_{\alpha\beta}. \tag{4}$$

Since the spins have been quantized along the x-axis, the spin–orbit coupling leads to scattering events always accompanied by spin-flip transitions.

The following analysis is simplified by introducing the usual four-component field operators [8, 11]:

$$\Psi_{\boldsymbol{k}} = \begin{bmatrix} c_{\boldsymbol{k}\uparrow} \\ c_{-\boldsymbol{k}\downarrow} \\ c^{\dagger}_{\boldsymbol{k}\uparrow} \\ c^{\dagger}_{-\boldsymbol{k}\downarrow} \end{bmatrix} \qquad \Psi^{\dagger}_{\boldsymbol{k}} = \left[c^{\dagger}_{\boldsymbol{k}\uparrow}, c^{\dagger}_{-\boldsymbol{k}\downarrow}, c_{\boldsymbol{k}\uparrow}, c_{-\boldsymbol{k}\downarrow} \right]. \tag{5}$$

From equations (1), (3) it is possible to evaluate the equation of motion of the field operator $\Psi_{\boldsymbol{k}}$ in imaginary time τ:

$$\frac{\mathrm{d}\Psi_{\boldsymbol{k}}}{\mathrm{d}\tau} = -\epsilon(\boldsymbol{k})\rho_3\Psi_{\boldsymbol{k}} - \Delta(\boldsymbol{k})\rho_2\tau_2\Psi_{\boldsymbol{k}} + I\rho_3\tau_3\Psi_{\boldsymbol{k}} - \sum_{\boldsymbol{k}',i} \mathrm{e}^{\mathrm{i}(\boldsymbol{k}-\boldsymbol{k}')\cdot\boldsymbol{R}_i} \left[v_{\mathrm{imp}}\rho_3 + \mathrm{i}\frac{v_{\mathrm{so}}}{k_{\mathrm{F}}^2}[\boldsymbol{k}\times\boldsymbol{k}']\cdot\hat{\boldsymbol{z}}\,\tau_1 \right] \Psi_{\boldsymbol{k}'} \tag{6}$$

where the products $\rho_i\tau_j$ are 4×4 matrices acting on the field operators (5). They are constructed by treating the Pauli matrices τ_j as elements of the Pauli matrices ρ_i as shown in the example below:

$$\rho_2\tau_2 = \begin{pmatrix} 0 & -\mathrm{i}\tau_2 \\ \mathrm{i}\tau_2 & 0 \end{pmatrix}. \tag{7}$$

Equation (6) permits us to evaluate the equation of motion of the generalized Green's function, defined as

$$G(\boldsymbol{k},\boldsymbol{k}';\tau) = -\langle T_\tau \Psi_{\boldsymbol{k}}(\tau)\Psi^{\dagger}_{\boldsymbol{k}'}(0)\rangle \tag{8}$$

where T_τ is the τ-order operator. It is straightforward to obtain from equations (6) and (8) the equation satisfied by the generalized Green's function in the Matsubara frequencies $\omega_n = (2n+1)\pi T$:

$$G(\boldsymbol{k},\boldsymbol{k}';\mathrm{i}\omega_n) = \delta_{\boldsymbol{k},\boldsymbol{k}'}G_0(\boldsymbol{k},\mathrm{i}\omega_n) + G_0(\boldsymbol{k},\mathrm{i}\omega_n)\sum_{\boldsymbol{k}''}\sum_i \mathrm{e}^{\mathrm{i}(\boldsymbol{k}-\boldsymbol{k}'')\cdot\boldsymbol{R}_i} V(\boldsymbol{k},\boldsymbol{k}'')G(\boldsymbol{k}'',\boldsymbol{k}';\mathrm{i}\omega_n) \tag{9}$$

where

$$V(\boldsymbol{k},\boldsymbol{k}'') = v_{\mathrm{imp}}\rho_3 + \mathrm{i}\frac{v_{\mathrm{so}}}{k_{\mathrm{F}}^2}[\boldsymbol{k}\times\boldsymbol{k}'']\cdot\hat{\boldsymbol{z}}\tau_1 \tag{10}$$

and

$$G_0(\boldsymbol{k},\mathrm{i}\omega_n) = [\mathrm{i}\omega_n - \epsilon(\boldsymbol{k})\rho_3 - \Delta(\boldsymbol{k})\rho_2\tau_2 - I\rho_3\sigma_3]^{-1} \tag{11}$$

is the Green's function in the absence of impurities.

The average over all the impurity configurations of equation (9) leads to the averaged Green's function $\bar{G}$ which satisfies the following Dyson equation [11]:

$$\bar{G}^{-1}(\boldsymbol{k},\mathrm{i}\omega_n) = G_0^{-1}(\boldsymbol{k},\mathrm{i}\omega_n) - \Sigma(\boldsymbol{k},\mathrm{i}\omega_n) \tag{12}$$

where Σ is the electron self-energy resulting from the averaging procedure. In this paper, v_{imp} and v_{so} are assumed to be sufficiently weak to justify a self-consistent Born approximation for the self-energy Σ. Because of the momentum dependence of the spin–orbit interaction, the Feynman diagrams describing the Born approximation do not involve impurity–spin–orbit mixed terms and Σ is given by the diagrams shown in figure 1. Therefore, using equation (10), the self-consistent Born approximation for Σ reads

$$\Sigma(\boldsymbol{k},\mathrm{i}\omega_n) = n\sum_{\boldsymbol{k}'} V(\boldsymbol{k},\boldsymbol{k}')\bar{G}(\boldsymbol{k}',\mathrm{i}\omega_n)V(\boldsymbol{k}',\boldsymbol{k})$$

$$= nv_{\mathrm{imp}}^2\sum_{\boldsymbol{k}'}\rho_3\bar{G}(\boldsymbol{k}',\mathrm{i}\omega_n)\rho_3 + n\frac{v_{\mathrm{so}}^2}{k_{\mathrm{F}}^4}\sum_{\boldsymbol{k}'}|\boldsymbol{k}\times\boldsymbol{k}'|^2\tau_1\bar{G}(\boldsymbol{k}',\mathrm{i}\omega_n)\tau_1 \tag{13}$$

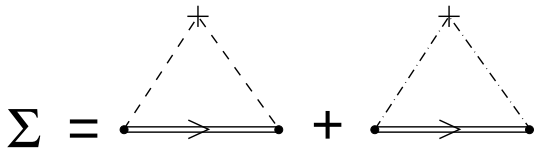

Figure 1. Feynman diagrams for the self-energy in the self-consistent Born approximation. The impurity and spin–orbit interactions are represented by dashed and dot–dashed lines, respectively.

where n is the concentration of impurities.

Equations (12) and (13) must be solved self-consistently and the solution can be written in terms of the following renormalized Green's function [8, 11, 12]:

$$\bar{G}^{-1}(\boldsymbol{k}, \mathrm{i}\omega_n) = \mathrm{i}(\tilde{\omega} - \mathrm{i}\tilde{I}\rho_3\sigma_3) - \rho_3(\tilde{\epsilon} - \mathrm{i}\tilde{\Lambda}\rho_3\sigma_3) - \rho_2\sigma_2(\tilde{\Delta} - \mathrm{i}\tilde{\Omega}\rho_3\sigma_3) \quad (14)$$

where for brevity the momentum and frequency dependence of the quantities with tildes has been omitted. The renormalized quantities can be calculated by substituting equation (14) into equations (12), (13). If there is particle–hole symmetry, the quasiparticle dispersion remains unaffected by the presence of impurities, i.e., $\tilde{\epsilon} = \epsilon(\boldsymbol{k})$ and $\tilde{\Lambda} = 0$. For the other quantities it is useful to introduce the variables $\tilde{\omega}_\pm$ and $\tilde{\Delta}_\pm$ defined by

$$\tilde{\omega}_\pm = \tilde{\omega} \pm \mathrm{i}\tilde{I} \qquad \tilde{\Delta}_\pm = \tilde{\Delta} \pm \mathrm{i}\tilde{\Omega}. \quad (15)$$

In this way the self-consistent equations become

$$\tilde{\omega}_\pm = \omega_n \pm \mathrm{i}I + nv_{\mathrm{imp}}^2 \sum_{\boldsymbol{k}'} \frac{\tilde{\omega}_\pm}{\epsilon(\boldsymbol{k}')^2 + \tilde{\Delta}_\pm^2 + \tilde{\omega}_\pm^2} + n\frac{v_{\mathrm{so}}^2}{k_{\mathrm{F}}^4} \sum_{\boldsymbol{k}'} \frac{|\boldsymbol{k} \times \boldsymbol{k}'|^2 \tilde{\omega}_\mp}{\epsilon(\boldsymbol{k}')^2 + \tilde{\Delta}_\mp^2 + \tilde{\omega}_\mp^2} \quad (16)$$

$$\tilde{\Delta}_\pm = \Delta(\boldsymbol{k}) + nv_{\mathrm{imp}}^2 \sum_{\boldsymbol{k}'} \frac{\tilde{\Delta}_\pm}{\epsilon(\boldsymbol{k}')^2 + \tilde{\Delta}_\pm^2 + \tilde{\omega}_\pm^2} + n\frac{v_{\mathrm{so}}^2}{k_{\mathrm{F}}^4} \sum_{\boldsymbol{k}'} \frac{|\boldsymbol{k} \times \boldsymbol{k}'|^2 \tilde{\Delta}_\mp}{\epsilon(\boldsymbol{k}')^2 + \tilde{\Delta}_\mp^2 + \tilde{\omega}_\mp^2}. \quad (17)$$

The summations over momenta are transformed into integrations over energy according to the usual procedure:

$$\sum_{\boldsymbol{k}'} \to V \int \frac{\mathrm{d}^2k'}{(2\pi)^2} \simeq N_0 \int_0^{2\pi} \frac{\mathrm{d}\phi'}{2\pi} \int \mathrm{d}\epsilon \quad (18)$$

where N_0 is the electronic density of states per spin state at the Fermi level. Performing the integration over the energy ϵ, equations (16) and (17) reduce to

$$\tilde{\omega}_\pm = \omega_n \pm \mathrm{i}I + \frac{1}{2\tau} \int \frac{\mathrm{d}\phi'}{2\pi} \frac{\tilde{\omega}_\pm}{[\tilde{\omega}_\pm^2 + \tilde{\Delta}_\pm(\phi')^2]^{1/2}} + \frac{1}{\tau_{\mathrm{so}}} \int \frac{\mathrm{d}\phi'}{2\pi} \frac{S(\phi, \phi')\tilde{\omega}_\mp}{[\tilde{\omega}_\mp^2 + \tilde{\Delta}_\mp(\phi')^2]^{1/2}} \quad (19)$$

$$\tilde{\Delta}_\pm(\phi) = \Delta(\phi) + \frac{1}{2\tau} \int \frac{\mathrm{d}\phi'}{2\pi} \frac{\tilde{\Delta}_\pm(\phi')}{[\tilde{\omega}_\pm^2 + \tilde{\Delta}_\pm(\phi')^2]^{1/2}} + \frac{1}{\tau_{\mathrm{so}}} \int \frac{\mathrm{d}\phi'}{2\pi} \frac{S(\phi, \phi')\tilde{\Delta}_\mp(\phi')}{[\tilde{\omega}_\mp^2 + \tilde{\Delta}_\mp(\phi')^2]^{1/2}} \quad (20)$$

where τ^{-1} and $(\tau_{\mathrm{so}})^{-1}$ are the scattering rates for the non-magnetic and spin–orbit impurities, respectively. They are given by

$$\frac{1}{\tau} = 2\pi n v_{\mathrm{imp}}^2 N_0 \qquad \frac{1}{\tau_{\mathrm{so}}} = \pi n v_{\mathrm{so}}^2 N_0. \quad (21)$$

In equations (19), (20), the function $S(\phi, \phi')$ stems from the angular dependence of the spin–orbit factor $|\hat{\boldsymbol{k}} \times \hat{\boldsymbol{k}}'|^2$ on defining ϕ and ϕ' as the polar angles of the vectors $\boldsymbol{k}$ and $\boldsymbol{k}'$, respectively. In explicit form, the function $S(\phi, \phi')$ is given by

$$S(\phi, \phi') = \cos(\phi)^2 \sin(\phi')^2 + \sin(\phi)^2 \cos(\phi')^2 - \frac{1}{2} \sin(2\phi) \sin(2\phi'). \quad (22)$$

The presence of such an angular function leads to important differences between non-magnetic and spin–orbit impurity effects also for zero magnetic field. In fact, non-magnetic impurities do not renormalize the gap function when this has d-wave symmetry [7] whereas the spin–orbit interaction, by means of the angular function $S(\phi, \phi')$, provides a finite renormalization. This can be readily seen by realizing that if $\Delta(\phi)$ is of the form given by equation (2), then a consistent solution of equation (20) is provided by setting $\tilde{\Delta}_\pm(\phi) = \tilde{\Delta}_\pm \cos(2\phi)$, where $\tilde{\Delta}_\pm$ is the solution of

$$\tilde{\Delta}_\pm = \Delta + \frac{1}{\tau_{so}} \int \frac{d\phi}{2\pi} \sin(\phi)^2 \frac{\tilde{\Delta}_\mp \cos(2\phi)}{[\tilde{\omega}_\mp^2 + \tilde{\Delta}_\mp^2 \cos(2\phi)^2]^{1/2}} \tag{23}$$

and, in the same way, equation (19) becomes

$$\tilde{\omega}_\pm = \omega_n \pm iI + \frac{1}{2\tau} \int \frac{d\phi}{2\pi} \frac{\tilde{\omega}_\pm}{[\tilde{\omega}_\pm^2 + \tilde{\Delta}_\pm^2 \cos(2\phi)^2]^{1/2}} + \frac{1}{\tau_{so}} \int \frac{d\phi}{2\pi} \sin(\phi)^2 \frac{\tilde{\omega}_\mp}{[\tilde{\omega}_\mp^2 + \tilde{\Delta}_\mp^2 \cos(2\phi)^2]^{1/2}}. \tag{24}$$

In obtaining equations (23), (24), we have used the identity

$$\int \frac{d\phi}{2\pi} \cos(\phi)^2 f[\cos(2\phi)] = \int \frac{d\phi}{2\pi} \sin(\phi)^2 f[-\cos(2\phi)] \tag{25}$$

where $f[\cos(2\phi)]$ is a general function of $\cos(2\phi)$.

As expected, the scalar impurity scattering contribution has disappeared from the gap renormalization (23). In contrast, the spin–orbit interaction modifies the gap function because of the presence of the angular function (22). Moreover, equations (23) and (24) are renormalized in a different way by v_{so} so, even at zero magnetic field, the spin–orbit interaction contributes to the thermodynamic and spectral properties of d-wave superconductors. In fact, all the measurable quantities can be expressed in terms of $\tilde{u}_\pm = \tilde{\omega}_\pm / \tilde{\Delta}_\pm$ [12] which from equations (23), (24) satisfies the following equation:

$$\tilde{u}_\pm = \frac{\omega_n \pm iI}{\Delta} + \frac{1}{2\Delta\tau} \int \frac{d\phi}{2\pi} \frac{\tilde{u}_\pm}{[\cos(2\phi)^2 + \tilde{u}_\pm^2]^{1/2}} + \frac{1}{\Delta\tau_{so}} \int \frac{d\phi}{2\pi} \sin(\phi)^2 \frac{\tilde{u}_\mp - \tilde{u}_\pm \cos(2\phi)}{[\cos(2\phi)^2 + \tilde{u}_\mp^2]^{1/2}}. \tag{26}$$

The above equation should be compared with the corresponding expression for the two-dimensional isotropic s-wave case which, on setting $\Delta(\phi) = \Delta$ in equations (19), (20), is found to be [4, 8, 12]

$$\tilde{u}_\pm = \frac{\omega_n \pm iI}{\Delta} + \frac{1}{2\Delta\tau_{so}} \frac{\tilde{u}_\mp - \tilde{u}_\pm}{[1 + \tilde{u}_\mp^2]^{1/2}} \tag{27}$$

where the contribution of the impurity scattering has vanished because of Anderson's theorem. When $H = 0$, equation (27) reduces to $\tilde{u}_+ = \tilde{u}_- = \omega_n/\Delta$ and does not depend on the spin–orbit scattering rate, while equation (26) still depends on τ and τ_{so}. In fact, in a d-wave superconductor, both the non-magnetic impurity and the spin–orbit scatterings are pair breaking and they tend to suppress superconductivity [9]. When $\boldsymbol{H} \neq 0$, one therefore expects the Zeeman response of a d-wave superconductor to differ qualitatively from that of an s-wave condensate.

3. Phase diagram

Equation (26) permits us to obtain all the information needed to calculate the phase diagram of a dirty d-wave superconductor in a Zeeman magnetic field. Let us start by considering the

self-consistent equation for the order parameter Δ:

$$\Delta = \frac{V_0}{4} T \sum_n \sum_{\boldsymbol{k}} \cos(2\phi)\, \mathrm{Tr}[\rho_2 \tau_2 \bar{G}(\boldsymbol{k}, \mathrm{i}\omega_n)] = \lambda \pi T \sum_n \int \frac{\mathrm{d}\phi}{2\pi}\, \mathrm{Re}\, \frac{\cos(2\phi)^2}{[\cos(2\phi)^2 + \tilde{u}_+^2]^{1/2}} \tag{28}$$

where V_0 is the pairing interaction and $\lambda = V_0 N_0$. The summation over the frequencies is implicitly assumed to be restricted by a cut-off energy. However, both the cut-off frequency and the pairing interaction can be absorbed in the definition of the critical temperature T_{c0} for a pure superconductor ($\tau^{-1} = 0$, $\tau_{so}^{-1} = 0$) without external magnetic field. In this way the gap equation can be rewritten as

$$\ln\left(\frac{T}{T_{c0}}\right) = 4\pi T \sum_{n \geqslant 0} \left\{ \int \frac{\mathrm{d}\phi}{2\pi}\, \mathrm{Re}\left(\frac{1}{\Delta} \frac{\cos(2\phi)^2}{[\cos(2\phi)^2 + \tilde{u}_+^2]^{1/2}} \right) - \frac{1}{2\omega_n} \right\}. \tag{29}$$

On the hypothesis that the transition to the normal state is of the second order (see below), the critical temperature T_c is obtained from equation (28) by setting $\Delta \to 0$ and it is given by

$$\ln\left(\frac{T_c}{T_{c0}}\right) = \psi\left(\frac{1}{2}\right) - \frac{1}{2}\left[\left(1 + \frac{1}{4\tau_{so} b}\right) \psi\left(\frac{1}{2} + a + \frac{b}{2\pi T_c}\right) + \left(1 - \frac{1}{4\tau_{so} b}\right) \psi\left(\frac{1}{2} + a - \frac{b}{2\pi T_c}\right) \right] \tag{30}$$

where $a = (\tau^{-1} + \tau_{so}^{-1})/4\pi T_c$ and $b = [1/(4\tau_{so})^2 - I^2]^{1/2}$, and ψ is the di-gamma function. When $I = \mu_B H = 0$, equation (30) reduces to

$$\ln\left(\frac{T_c}{T_{c0}}\right) = \psi\left(\frac{1}{2}\right) - \psi\left(\frac{1}{2} + \frac{1}{4\pi T_c \tau} + \frac{3}{4} \frac{1}{2\pi T_c \tau_{so}}\right) \tag{31}$$

which coincides with the result obtained in reference [9] in the weak-scattering limit†. Equation (31) shows that, even at zero magnetic field, the spin–orbit scattering contributes together with the non-magnetic impurity scattering to the suppression of T_c.

For large enough values of the external magnetic field, the transition to the normal state becomes of first order [5]. This situation is studied by evaluating the difference in free energy between the superconducting and the normal states, $\Delta F = F_s - F_n$. If, on raising the temperature and/or the magnetic field, ΔF changes sign while Δ remains finite, then the system undergoes a first-order phase transition to the normal state with critical field H_c and T_c determined by $\Delta F = 0$ [4]. Following reference [12], ΔF is obtained as

$$\Delta F = \int_0^{V_0} \mathrm{d}V_0\, \Delta^2 \tag{32}$$

and by using equations (26), (28), one readily finds

$$\Delta F = -N_0 \Delta\, 2\pi T \sum_{n \geqslant 0} \int \frac{\mathrm{d}\phi}{2\pi}\, \mathrm{Re} \left\{ 2[\cos(2\phi)^2 + \tilde{u}_+^2]^{1/2} - 2\tilde{u}_+ - \frac{\cos(2\phi)^2}{[\cos(2\phi)^2 + \tilde{u}_+^2]^{1/2}} \right\}. \tag{33}$$

The numerical solutions of equations (30) and (33) are shown in figure 2 for the pure limit and, for comparison, the d-wave solution is plotted together with the s-wave one. In the phase diagram, the solid and dashed lines are solutions of equations (30) and (33), respectively. For

† In reference [9] a different notation has been used in which the impurity potential is parametrized by $\Gamma = n/(\pi N_0)$ and $c = 1/(\pi N_0 v_{imp})$ and the spin–orbit interaction is parametrized as $v_{so} = \Delta g v_{imp}$, where Δg is the shift of the electronic g-factor. Therefore, on using equation (21), $1/(2\tau) = \Gamma/c^2$ and $1/\tau_{so} = \Gamma(\Delta g/c)^2$.

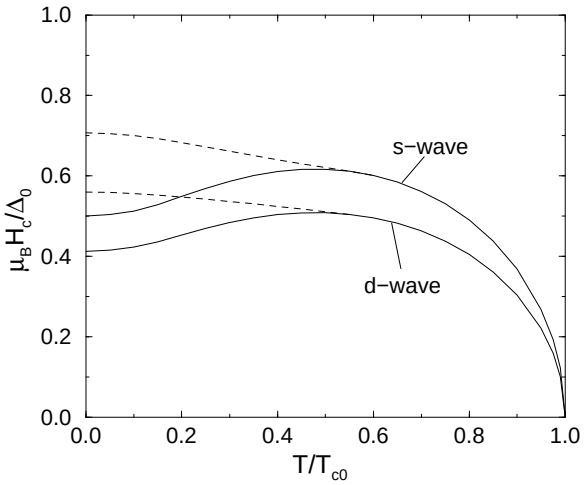

Figure 2. The phase diagram for pure s-wave and d-wave superconductors in the presence of a Zeeman magnetic field. Δ_0 and T_{c0} are the order parameter and the critical temperature without the external magnetic field, respectively. For $T/T_{c0} > 0.56$ the solid lines are the second-order phase boundary between the normal (above the solid lines) and the superconducting (below the solid lines) states. For $T/T_{c0} < 0.56$ both the s-wave and the d-wave states show a first-order transition to the normal state marked by the dashed lines. In this region, the solid lines represent the supercooling fields.

both d waves and s waves, the transition to the normal state is of second order for $T/T_{c0} \geqslant 0.56$ [1, 2, 6] while for lower temperatures the transition, marked by dashed lines, becomes of first order. For $T/T_{c0} < 0.56$ the solid lines represent the supercooling field [1, 2, 4]. As already stated in the introduction, at zero temperature the first-order transition to the normal state is obtained for critical fields $\mu_B H_c/\Delta_0 = 1/\sqrt{2}$ [5] for s waves and $\mu_B H_c/\Delta_0 \simeq 0.56$ for d waves [1,2]. In this paper, the Fulde–Ferrel–Larkin–Ovchinnikov state [13] which appears at low temperatures has not been considered since disorder tends to restore the zero-momentum pairing [14]. For the pure d-wave case, the reader can find the phase diagram including the non-zero-momentum pairing state in reference [1].

Although for the pure limit the phase diagrams of the Zeeman responses of s-wave and d-wave superconductors are qualitatively similar, they drastically differ when the coupling to the non-magnetic and spin–orbit impurity scatterings is switched on. In figures 3 and 4, the phase diagrams for s-wave and d-wave superconductors are plotted for finite values of τ^{-1} and τ_{so}^{-1}. In both figures, the impurity scattering parameter $b_n = 1/(2\Delta_0\tau)$ is set equal to 0.1, while the spin–orbit scattering parameter $b_{so} = 1/(2\Delta_0\tau_{so})$ assumes four different values: $b_{so} = 0, 0.06, 0.12, 0.16$. In the s-wave case, figure 3, the phase diagram is insensitive to $b_n \neq 0$, while finite values of b_{so} enhance the critical field for all temperatures. Moreover, the temperature interval of first-order phase transition (dashed lines) decreases as b_{so} increases and for $b_{so} > 2.32$ the transition becomes continuous for all temperatures [4]. This behaviour is due to the spin-mixing effect of the spin–orbit interaction which lowers the Zeeman response and consequently the depairing effect of the magnetic field. On the other hand, in the d-wave case shown in figure 4, the spin–orbit scattering is pair breaking and for $b_{so} > 0$ the critical field is lowered. This situation can be understood by realizing that finite values of b_{so} lead to a weakening of the superconducting state [9] with the result that, with respect to the $b_{so} = 0$ case, lower values of H are needed to suppress the superconductivity completely. Another striking

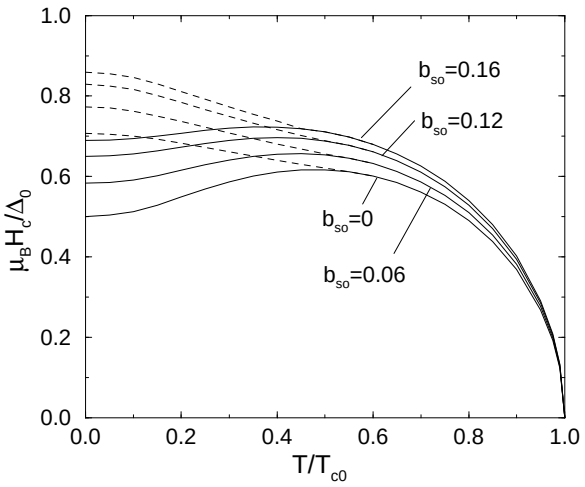

Figure 3. The phase diagram for an s-wave superconductor with impurity and spin–orbit scattering centres. The critical field is unaffected by the impurity potential, while it increases on increasing the spin–orbit scattering parameter $b_{so} = 1/(2\Delta_0\tau_{so})$ where Δ_0 is the order parameter in the pure limit without magnetic field. The solid and dashed lines have the same meaning as in figure 2.

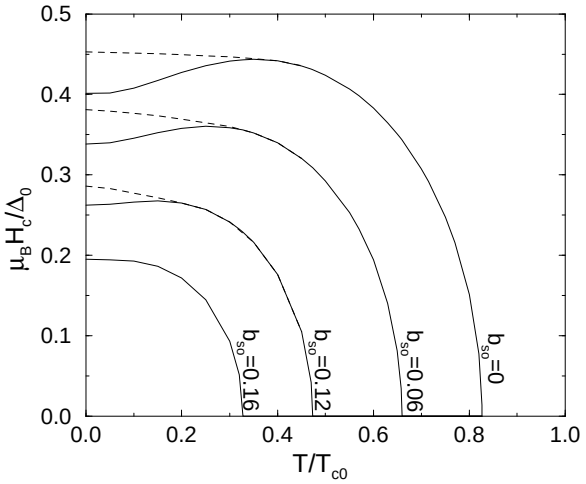

Figure 4. The phase diagram for a d-wave superconductor with impurity and spin–orbit scattering centres. The impurity scattering parameter is $b_n = 1/(2\Delta_0\tau) = 0.1$ where Δ_0 is the order parameter in the pure limit without magnetic field. The solid and dashed lines have the same meaning as in figure 2. Note that, contrary to the case shown in figure 3, for $b_{so} = 0.16$ the transition to the normal state is already of second order for the whole temperature range.

feature is that, due to the nodes of the d-wave order parameter, the b_{so}-dependence of the phase diagram is much stronger than for the s-wave case. In fact, for $b_{so} = 0.16$ there is already no signature for a first-order transition whereas for an s-wave superconductor the first-order transition disappears only for $b_{so} > 2.36$, i.e., a difference of one order of magnitude.

It is important to stress that the remarkable difference between the d-wave and s-wave phase diagrams has been obtained in the Born limit of non-magnetic and spin–orbit impurity scatterings. However, it is well known that in high-T_c superconductors the effect of disorder is best described by the strongly resonant limit of the impurity potential, so the Born approximation may be inadequate. In practice, one should formulate the Zeeman response by employing the t-matrix approximation for both the non-magnetic and the spin–orbit potentials.

Such a calculation has already been reported in reference [9] for zero external magnetic field. The generalization for $H \neq 0$ is currently under investigation and the results reported here may provide a useful tool for testing the more general t-matrix solution.

4. Density of states

With the effect of $b_{\rm n}$ and $b_{\rm so}$ on the phase diagram having been described, it is interesting to investigate also how the spectral properties are modified. To this end, equation (26) must be analytically continued to the real axis by setting $\mathrm{i}\tilde{u}_\pm \to u_\pm$ and $\mathrm{i}\omega_n \to \omega$. In this way, the quasiparticle density of states (DOS) per spin direction in units of the normal state DOS N_0 can be calculated using the following expression:

$$\rho_\pm(\omega) = \frac{N_\pm(\omega)}{N_0} = \mathrm{sgn}(\omega) \int \frac{\mathrm{d}\phi}{2\pi}\, \mathrm{Re}\, \frac{u_\pm}{[u_\pm^2 - \cos(2\phi)^2]^{1/2}}. \tag{34}$$

In figure 5 we report the quasiparticle DOS for $I = \mu_{\rm B}H = 0.15\Delta_0$, $b_{\rm n} = 0.1$, and different values of the spin–orbit parameter $b_{\rm so}$. For clarity, the curves with $b_{\rm so} \neq 0$ have been vertically shifted by 0.7, 2×0.7, and 3×0.7 with respect to those with $b_{\rm so} = 0$. For $b_{\rm so} = 0$, the two DOS per spin state, ρ_+ (dashed lines) and ρ_- (solid lines), show a clear Zeeman splitting and for $\omega = 0$ the total DOS $\rho = \rho_+ + \rho_-$ is different from zero as expected for a d-wave superconductor. For $b_{\rm so} > 0$ the total DOS at $\omega = 0$ is enhanced at the expense of the coherence peaks which show a decrease of spectral weight. Moreover, at $\omega \simeq \mu_{\rm B}H$, ρ_- develops a structure (marked by the arrows) which becomes a peak at $b_{\rm so} = 0.16$. Such a structure is even more clearly visible in figure 6 where $\rho_\pm$ is plotted for $b_{\rm n} = 0.1$, $b_{\rm so} = 0.06$,

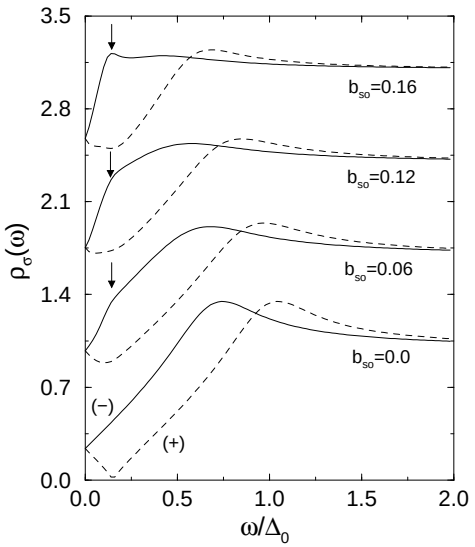

Figure 5. The Zeeman-split quasiparticle densities of states $\rho_+(\omega)$ (dashed lines) and $\rho_-(\omega)$ (solid lines) for a d-wave superconductor with $b_{\rm n} = 0.1$, $\mu_{\rm B}H/\Delta_0 = 0.15$, and different values of the spin–orbit scattering parameter $b_{\rm so}$. The curves for different values of $b_{\rm so}$ are vertically shifted by multiples of 0.7. Note the structure (marked by the arrows) at $\omega \simeq \mu_{\rm B}H$ which develops as $b_{\rm so}$ increases.

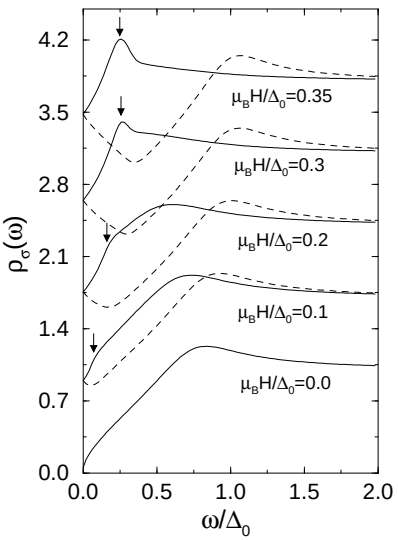

Figure 6. The Zeeman-split quasiparticle densities of states $\rho_+(\omega)$ (dashed lines) and $\rho_-(\omega)$ (solid lines) for a d-wave superconductor with $b_{\rm n} = 0.1$, $b_{\rm so} = 0.06$, and different values of the external magnetic field. The curves for different values of H are vertically shifted by multiples of 0.7. The arrows indicate the resonant structure which develops a peak for $\mu_{\rm B}H > 0.3$ (see the text).

and different values of the external magnetic field. The origin of this peak can be understood from the following reasoning. At the Fermi wave-vector, and for a pure superconductor, the quasiparticle energies for spin up and down are $E_{\pm}(\phi) = \Delta|\cos(2\phi)| \pm \mu_B H$ and, therefore, depending on the values of H and Δ, two quasiparticles with different spin orientations and angles ϕ can have equal energies. For example, for $\phi_1 = 0$ and $\phi_2 = \pi/4$, the two energies $E_-(\phi_1)$ and $E_+(\phi_2)$ are equal to $\omega = \mu_B H$ if $\Delta = 2\mu_B H$. Since the spin–orbit potential connects quasiparticle states with different spin orientations but equal energies, the two states $E_-(\phi_1)$ and $E_+(\phi_2)$ are coupled by the spin–orbit interaction and an enhanced signal should be expected at $\omega \simeq \mu_B H$. Note in fact that in figure 6 the low-energy peak is more pronounced for $\mu_B H = 0.35\Delta_0$ where, since $\Delta \simeq 0.68\Delta_0$, the condition $\Delta = 2\mu_B H$ is nearly fulfilled.

5. Conclusions

In conclusion, it has been shown within the Born approximation that the presence of impurity and spin–orbit scattering centres strongly affects the Zeeman response of a d-wave superconductor. Both the phase diagram and the quasiparticle density of states show features qualitatively different from those of an s-wave superconductor. In fact, on increasing the value of the spin–orbit scattering parameter $b_{so} = 1/(2\Delta_0\tau_{so})$ the critical field H_c is strongly lowered whereas in an s-wave superconductor H_c increases. Moreover, the influence of b_{so} on the superconducting state is much stronger for the d-wave symmetry. Concerning the spectral properties, the Zeeman-split density of states of a d-wave superconductor shows interesting features which are missing in an s-wave superconductor. In fact, for sufficiently large values of b_{so} and/or H a resonant peak develops at energies close to $\mu_B H$. The origin of this feature is given by the anisotropy of the order parameter and the spin-flip transitions due to the spin–orbit scattering. An important open question concerns the possibility of going beyond the Born approximation and employing a t-matrix approach for the Zeeman response in the presence of impurity and spin–orbit scattering centres in order to test the solidity of the results presented here.

References

[1] Yang K and Sondhi S L 1998 *Phys. Rev.* B **57** 8566
[2] Won H, Jang H and Maki K 1999 *Preprint* cond-mat/9901252
[3] Ghosh H 1999 *Phys. Rev.* B **60** 3538
[4] Fulde P 1973 *Adv. Phys.* **22** 667
[5] Clogston A M 1962 *Phys. Rev. Lett.* **3** 266
Chandrasekhar B S 1962 *Appl. Phys. Lett.* **1** 7
[6] Sarma G 1963 *J. Phys. Chem. Solids* **24** 1029
[7] Hirschfeld P J and Goldenfeld N 1993 *Phys. Rev.* B **48** 4219
Sun Y and Maki K 1995 *Phys. Rev.* B **51** 6059
[8] Fulde P and Maki K 1966 *Phys. Rev.* **141** 275
[9] Grimaldi C 1999 *Europhys. Lett.* **48** 306
[10] Elliott R J 1954 *Phys. Rev.* **96** 266
[11] Rickayzen G 1980 *Green's Functions and Condensed Matter* (London: Academic)
[12] Maki K 1969 *Superconductivity* vol 2, ed R D Parks (New York: Dekker) p 1035
[13] Fulde P and Ferrel R A 1964 *Phys. Rev.* **135** A550
Larkin A I and Ovchinnikov Yu N 1965 *Sov. Phys.–JETP* **20** 762
[14] Grunberg L W and Gunther L 1966 *Phys. Rev. Lett.* **16** 996